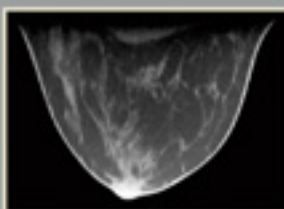
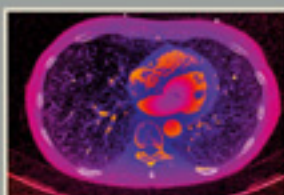
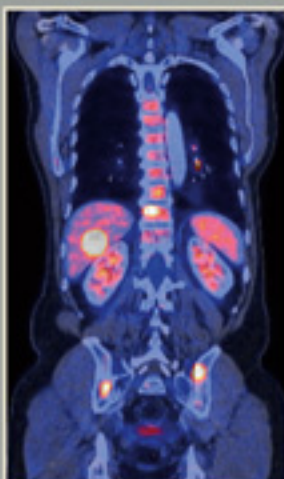


Willi A. Kalender

Computed Tomography

Fundamentals
System Technology
Image Quality
Applications

3rd Edition



Dual Energy CT, PET/CT, Breast CT
Perfusion CT, Cardiac CT, Micro CT
3D Dose Distribution, Whole Body CT
All pictures on DVD



PUBLICIS

Kalender Computed Tomography

The author

Willi A. Kalender, born in 1949, studied physics and medical physics in Bonn, Germany, and at the University of Wisconsin, Madison, Wisconsin. Active from 1979 to 1995, i.e. for exactly 16 years, in CT research & development at Siemens Medical Solutions in Erlangen, Germany. Professor and chairman of the Institute of Medical Physics (IMP) at the University Erlangen-Nuremberg since 1995 where he completed another 16 years of CT research and development by now.

To obtain further and topical information on the author or further projects and work, especially related to new developments in CT, please visit our website www.imp.uni-erlangen.de at any time.

Computed Tomography

Fundamentals, System Technology,
Image Quality, Applications

by Willi A. Kalender

3rd revised edition, 2011

Publicis Publishing

Bibliographic information published by the Deutsche Nationalbibliothek
The Deutsche Nationalbibliothek lists this publication in
the Deutsche Nationalbibliografie; detailed bibliographic data
are available in the Internet at <http://dnb.d-nb.de>.

The author and publisher have taken great care with all texts and illustrations in this book. Nevertheless, errors can never be completely avoided. The publisher and author accept no liability, regardless of legal basis. Designations used in this book may be trademarks whose use by third parties for their own purposes could violate the rights of the owners.

www.publicis-books.de

Editor: Dorit Gunia, Publicis Publishing, Erlangen
dorit.gunia@publicis.de

ISBN 978-3-89578-317-3

Publisher: Publicis Publishing, Erlangen
© 2011 by Publicis Erlangen, Zweigniederlassung der PWW GmbH

This publication and all parts thereof are protected by copyright.
Any use of it outside the strict provisions of the copyright law without the consent of the publisher is forbidden and will incur penalties. This applies particularly to reproduction, translation, microfilming or other processing, and to storage or processing in electronic systems. It also applies to the use of individual illustrations or extracts from the text.

Printed in Germany

Preface

X-ray computed tomography (CT) which was introduced to medicine in the early 1970s brought slice imaging into wide use for the first time and represented its breakthrough. Today, CT is an essential part of radiological diagnostics and can be seen as a mature and clinically accepted procedure. It has supplemented or replaced classical x-ray imaging in many areas and has provided many valuable new applications.

A rapid technical development phase in the seventies was followed by an uneventful phase with no essential highlights in the eighties. This was partly caused by the expectation that the importance of CT would decrease successively due to the introduction of magnetic resonance (MR) tomography. Contrary to these expectations, CT started a phase of rapid technical development and again broadening its application spectrum in the nineties: The development of spiral CT and the transition from scanning single slices to the rapid scanning of complete volumes made CT attractive again and has led to decisive developments in technical and in clinical perspectives such as rotation times in the subsecond range and multi-row detector systems. The introduction of even wider detector systems, of dual source CT (DSCT) technology and dual energy scanning augmented these developments further and constituted the high points in the 2000s.

The present book is intended to describe technical and physical aspects of computed tomography, from sequential single-slice scanning to volume scanning by cone-beam spiral CT (MSCT). The fundamentals of CT are described in detail in the first chapter for “CT novices” in an illustrative manner. Readers familiar with this material may skip this chapter or refresh their knowledge by following the figures. Mathematical principles which are not required for the understanding of the following chapters are summarized as an appendix in chapter 9.

In addition to the necessary CT basics, the most recent developments and future-oriented considerations are presented in depth in chapters 2 to 4. Chapter 2 is dedicated to technical concepts in CT and the corresponding apparatus and scan modes, chapter 3 to spiral CT and chapter 4 to image quality considerations. The focus is always on problems relevant to the user of CT equipment. In particular, this includes the potential and the results of the newest technology and the corresponding scan and reconstruction options. The

routine availability of high isotropic resolution in all three dimensions is the eminent result. In view of the high topical interest, DSCT technology, performance and respective applications are addressed in detail in several sections. Sub-second high-pitch sub-mSv spiral CT scanning of the heart certainly is one of the highlights.

In view of the importance of radiation protection, questions regarding dose and possibilities for patient dose reduction are discussed separately in depth in chapter 5. The possibilities for dose reduction are emphasized, and concepts such as tube current modulation and an automatic exposure control for CT are explained. Such measures to reduce dose and to offer information on actual organ dose values should free CT from the generally held misconception of being a “high dose modality”. Effective dose values for typical CT examinations are on the order of magnitude of the natural background radiation per year as will be pointed out in detail.

2D and 3D approaches to display, to visualize and to diagnose CT images are explained in chapter 6. Interactive approaches continuously gaining importance for the data volumes encountered today are also illustrated by examples and offered on the DVD. In chapter 7, some fundamental remarks on and clinical examples for special applications follow with CT imaging of the heart and dual energy CT as two prominent examples being described in detail.

Chapter 8 offers an assessment of the prospects for future developments in CT. Technology, in particular potential detector developments, and applications are addressed. Dedicated CT of the breast, a new application to which the author assigns great potential, will serve as an example for this discussion. I hope that some of the predictions will prove to be true in the foreseeable future. I also hope that surprising new developments will arise that are not expected today. After all, CT is alive!

The material in this book is supported by image examples, video clips and the possibility of interactive exercises for image display and processing on the enclosed DVD. The respective supplements are indicated in the text. Example images for most body regions and some volume data sets can be loaded, windowed, magnified and viewed interactively. For “novices” – such as students or colleagues working in other fields who do not have easy access to a CT scanner or to CT data – this offers the possibility to familiarize themselves with results of CT imaging under realistic conditions. To appreciate all details in some of the figures showing clinical examples, it may be of help to look them up on the DVD. The DVD includes all figures of this book in digital form, i.e. in full quality. The feedback on the previous editions was very positive with many inquiries if the figures are free for use in your own presentations, teaching materials or else. That is exactly the

intention. For inclusion in published materials the publisher demands that you reference the book as the source of the material.

The book is addressed to a wide interdisciplinary readership in an effort to explain both the fundamentals and applications of CT. Consequently, the focus is on physics and technology, whereas radiological aspects are addressed only marginally. There is no requirement for special prior knowledge. Important CT terms are assembled in the glossary and defined briefly. With respect to detail problems or questions, relevant literature is referenced. There is no claim or effort though to provide a complete bibliography in order to keep this textbook self-explanatory as much as is possible. Whether the stated goals have been achieved remains open to the judgement of the reader. The author is open to suggestions, comments and criticism at any time and hopes that this 3rd edition of the textbook will meet with similar approval as the first two.

Have fun reading about computed tomography.

Erlangen, March 2011

Willi Kalender

Acknowledgements

It is not possible to mention all those by name who have contributed directly or indirectly to the generation of all the material in and to the completion of this book. This would have to include the many colleagues and partners in cooperation who supported me during more than three decades of work in CT development and who were available for many discussions.

Many of the newer CT images in this book and on the DVD have been generated on the SOMATOM Definition Flash which was provided to the Institute of Medical Physics (IMP) in 2008 by Siemens Healthcare for experimental and clinical work. I would like to explicitly acknowledge this support and the willingness of many colleagues at Siemens to cooperate on numerous projects. The results, e.g. on dose reduction and special CT applications, speak for the success of this cooperation.

Many colleagues from the Institute of Radiology of the University of Erlangen, under the direction of Michael Uder, have been excellent partners in the most recent CT projects. I would like to thank especially Arnd Dörfler, Michael Lell, Sedat Alibek and Stephan Achenbach for selecting and providing the clinical and cardiac CT images. Torsten Kuwert, director of the Nuclear Medicine Department, contributed the PET/CT and SPECT/CT cases. Mary Ellen Jafari and José Hernandez helped me with careful reviews of chapter 5. John Boone, pioneer in CT of the breast, contributed images and ideas for this fascinating novel topic presented in chapter 8.

I am particularly grateful to the coworkers at my own institute who have supported me during project “CT – the book” in relaxed manner, with constructive criticism and tireless efforts: thanks are due to Marie-Theres Reim for help with figures and text layout and to Felix Althoff, Marcel Beister, Paul Deak, Klaus Engelke, Martin Hupfer, Daniel Kolditz, Yiannis Kyriakou, Tristan Nowak, Yulia Smal, Sabrina Vollmar and Michaela Weigel for reviewing single chapters. I owe special thanks to Marc Kachelrieß for many helpful discussions and for providing his lecture notes as the basis for chapter 9. Should you be interested in learning about the persons behind these names, you can find further information under www.imp.uni-erlangen.de/team.

I am most grateful of all to my wife Marlene, who also tolerated and supported the project “CT – the book” in relaxed manner as usual and with valuable efforts to turn my personal English into something closer to standard English.

Contents

Historical Overview	14
1 Principles of Computed Tomography	18
1.1 General Considerations on Slice Imaging	18
1.1.1 Computed Tomography – a Digital Modality	18
1.1.2 Why Do Slice Images Offer Higher Contrast?	21
1.2 Basic Principles of CT	23
1.2.1 What Do We Measure in CT?	24
1.2.2 How Do We Measure an Object in CT?	26
1.2.3 How Do We Compute a CT Image?	27
1.2.4 What Is Displayed in CT Images?	31
2 Technical Concepts	37
2.1 Phases of Development and Goals	37
2.1.1 The Seventies – from Head to Whole Body Scanning	37
2.1.2 The Eighties – Fast Scanning of Single Slices	39
2.1.3 The Nineties – Fast Volume Scanning	40
2.1.4 The 2000s – Diversity and Even Faster Volume Scanning	41
2.1.5 The 2010s will be the Decade of Sub-mSv CT!	42
2.2 Standard Scanner Configuration	42
2.2.1 Mechanical Design	42
2.2.2 X-ray Components	47
2.2.3 Collimators and Filtration	51
2.2.4 Detector Systems	53
2.3 Scan Modes and Scan Parameters	64
2.3.1 Survey Radiographs	64
2.3.2 Scanning Single Sections – Sequential CT	65
2.3.3 Scanning Single Sections – “Step and Shoot” Modes	66
2.3.4 Material-Selective Imaging – Dual-Energy CT	67
2.3.5 Serial Scanning – Dynamic CT	67
2.3.6 CT Fluoroscopy – Interventional CT	68
2.3.7 Volume Scanning – Spiral CT	68
2.3.8 Volume Scanning – Cone-beam CT	69
2.4 Special Scanner Concepts	71
2.4.1 Electron Beam CT	72

2.4.2	The “Dynamic Spatial Reconstructor”	73
2.4.3	Flat Detector CT Scanners	74
2.4.4	PET/CT Combination Scanners	79
2.4.5	SPECT/CT Combination Scanners	81
2.4.6	Dual Source CT	83
3	Spiral CT	85
3.1	First Considerations and Efforts	85
3.2	Scanning Principle and Techniques in Spiral CT	87
3.3	Image Reconstruction in Spiral CT	90
3.3.1	Basic Approach to z -Interpolation (360° LI)	91
3.3.2	z -Interpolation Using Data Rebinning (180° LI)	92
3.3.3	Variations of 180° z -Interpolation Algorithms	94
3.4	Considerations for Multi-slice Spiral CT	97
3.4.1	z -Interpolation in Multi-slice Spiral CT (180° MLI)	97
3.4.2	z -Filtering in Multi-slice Spiral CT (180° MFI)	97
3.4.3	ECG-correlated Cardiac Imaging	100
3.5	Considerations for Cone-beam Spiral CT	102
3.5.1	Approaches for up to 64 Slices	102
3.5.2	Approaches for 64 Slices and more	106
3.5.3	High-pitch Dual Source CT Spiral Scanning	108
4	Image Quality	111
4.1	Variables and Procedures for Sequential CT	112
4.1.1	CT Values, Uniformity, Contrast and Linearity	112
4.1.2	Pixel Noise	114
4.1.3	Spatial Resolution – Resolution at High Contrast	116
4.1.4	Contrast Resolution – Resolution at Low Contrast	128
4.1.5	Artifacts	130
4.2	Variables and Procedures for Spiral CT	134
4.2.1	General Considerations	134
4.2.2	Pixel Noise	135
4.2.3	Slice Sensitivity Profiles	137
4.2.4	Resolution in the z -Direction	140
4.2.5	Considerations for Multi-slice Spiral CT	146
4.2.6	Considerations for Cone-beam Spiral CT	148
4.2.7	Artifacts in Spiral CT	151
4.2.8	The Effect of Finer Sampling in the z -Direction	153
4.2.9	Performance of Dual Source CT	156
4.3	Considerations for Flat Detector CT	157
4.3.1	Image quality considerations for C-arm-based FDCT	158
4.3.2	Image quality considerations for FDCT of the facial skull	162

4.3.3 Efforts at artifact reduction in FDCT	164
4.4 Total System Performance	168
4.4.1 The Interdependence of Noise, Dose and Resolution	168
4.4.2 Figures of Merit	171
4.5 Acceptance Test and Constancy Test	172
5 Dose	175
5.1 CT – the High Dose Myth	175
5.2 Technical Parameters for Dose Measurement	178
5.2.1 Dose Distributions in Sequential Single-slice Scans	178
5.2.2 Stray Radiation	186
5.2.3 Additional Considerations for Spiral CT Scans	187
5.2.4 Additional Considerations for Wide Detectors	189
5.2.5 CTDI Concepts for Wide Detectors	190
5.2.6 Dose Reference Levels for CT	192
5.2.7 Issues with CTDI	193
5.3 Patient Dose in CT	194
5.3.1 Influence of Scanning Parameters on the Patient Dose	194
5.3.2 Influence of Spiral CT on Patient Dose	196
5.3.3 Estimation of Organ Dose Values and Effective Dose	197
5.3.4 Estimation of Effective Dose	201
5.3.5 Issues with the determination of patient dose	207
5.4 Possibilities for Reducing the Dose Further	208
5.4.1 Influence by the Examiner	208
5.4.2 Technical Measures and New Approaches	210
5.5 How shall we deal with the discussion of dose?	222
5.5.1 Further Optimization of CT Systems	223
5.5.2 Information about Dose, Benefits and Risks	224
5.5.3 The Author’s Summing up and Recommendations	228
6 Processing and Visualization of Images	230
6.1 Simple Image Processing and Evaluation Procedures	230
6.2 Two-dimensional Displays	231
6.3 Three-dimensional Displays	233
6.3.1 Surface Displays	234
6.3.2 Projection Displays	236
6.3.3 Volume Rendering Techniques	237
6.3.4 Virtual Endoscopy	238
6.3.5 Recommendations on the Choice of 3D Display Methods	239
6.4 How to handle all the Images	242

7 Special Applications	245
7.1 General Considerations	245
7.2 Quantitative CT	246
7.3 Phase-selective Imaging of the Heart	250
7.3.1 Prospective Triggering in Sequential CT	251
7.3.2 Retrospective Gating in Spiral CT	252
7.3.3 High-pitch Spiral Dual Source CT with Prospective Triggering	254
7.3.4 Coronary Calcium Measurements with CT	255
7.4 Dual Energy CT	257
7.4.1 Basic physics of DECT	258
7.4.2 Technical solutions	263
7.4.3 DECT applications	265
7.5 Navigated Image-guided Interventions	268
7.6 Pre-clinical Imaging with CT (Micro-CT)	272
7.6.1 Micro-CT in-vitro imaging	272
7.6.2 Micro-CT in-vivo imaging	275
7.6.3 Quality control and dose assessment	278
7.7 Assessment of Tissue Perfusion with CT	282
7.7.1 Brain perfusion measurements in clinical CT	282
7.7.2 Alternative approaches to perfusion assessment by CT	285
7.7.3 Considerations regarding quality control and dose	287
8 The Future of CT	290
8.1 General considerations	291
8.2 Developments of technologies	292
8.3 Features of a dedicated breast CT scanner	294
8.4 Conclusions	302
9 Mathematical Aspects of Image Reconstruction	305
9.1 2D Image Reconstruction	307
9.1.1 Definition of 2D Parallel Projections	307
9.1.2 Reconstruction of Parallel Data	308
9.1.3 Parallel-Beam FBP	310
9.1.4 Definition of 2D Fan-Beam Projections	311
9.1.5 Fan-Beam FBP	312
9.1.6 Fan-Beam FBP for Equiangular Fans	313
9.1.7 Rebinning	315
9.1.8 Rebinning of Equiangular Fan-Beam Data	316
9.2 3D Image Reconstruction	316
9.2.1 Definition of Cone-Beam Projections	317

9.2.2 The Feldkamp Algorithm	318
9.2.3 EPBP, a Feldkamp-Type Algorithm	319
9.2.4 Single-Slice Rebinning Algorithms	322
9.2.5 Exact 3D Reconstruction from Cone-Beam Projections	324
References	329
Abbreviations and Symbols	346
Glossary	350
Index Terms	370

Historical Overview

“If we give free rein to our fantasy and imagine perfecting the new photographic process with the aid of Crookes’ tube until one part of the soft-tissue structures of the human body remains transparent and a layer located underneath can be imaged on the plate, this would be of invaluable assistance in diagnosing innumerable diseases not directly associated with bone structures.”

Translation of an excerpt from the “Frankfurter Zeitung”, January 7, 1896.

Ideas and concepts for tomographic imaging with x-rays were developed early. The unknown author of the above article appearing in the feature supplement of the “Frankfurter Zeitung” expressed truly prophetic thoughts only a few days after the first reports were published on Roentgen’s discovery of x-rays and prior to their first medical use. We do not know what the author had in mind when he conceived the possibility of displaying “... the soft tissue structures ... and a layer located underneath ...”. It was certainly not computed tomography as we know it today. Perhaps he wished to obtain a view similar to that with an anatomical preparation after superimposed layers of tissue have been removed. His assessment that “... this would be of invaluable assistance in diagnosing innumerable diseases not directly associated with bone structures” was in any case correct. One should, however, avoid over-interpretation of this quotation; the development of tomography, modern methods of reconstructing digital images, and today’s powerful computers were as yet undreamed of.

Computed tomography (CT) first became feasible with the development of modern computer technology in the sixties, but some of the ideas on which it is based can be traced back to the first half of this century. In 1917 the Bohemian mathematician J.H. Radon [Radon, 1917] proved in a research paper of fundamental importance that the distribution of a material or material property in an object layer can be calculated if the integral values along any number of lines passing through the same layer are known. The first applications of this theory were developed for radioastronomy by Bracewell in 1956 [Bracewell, 1956], but they met with little response and were not exploited for medical purposes.



Figure 1

Godfrey N. Hounsfield, the English engineer who developed the first CT scanner and received the Nobel Prize in medicine in 1979 together with the physicist A.M. Cormack.

The first experiments on medical applications of this type of reconstructive tomography were carried out by the physicist A.M. Cormack, who worked on improving radiotherapy planning at Groote Schuur Hospital, Cape Town, South Africa. Between 1957 and 1963, and without knowledge of previous studies, he developed a method of calculating radiation absorption distributions in the human body based on transmission measurements [Cormack, 1963]. He postulated for radiological applications that it must be possible to display even the most minute absorption differences, i.e. different soft-tissue structures. However, he never had occasion to put his theory into practice and first learned of Radon's work much later, a fact that he regretted by stating that earlier access to this knowledge would have saved him a lot of work. While familiarizing himself with Radon's work, Cormack discovered that Radon had himself been unaware of even earlier work on the subject by the Dutch physicist H.A. Lorentz, who had already proposed a solution of the mathematical problem for the 3D case in 1905 [Cormack, 1992].

A successful practical implementation of this theory was first achieved in 1972 by the English engineer G.N. Hounsfield, who is now generally recognized as the inventor of computed tomography [Hounsfield, 1973]. Like his predecessors, Hounsfield worked without knowledge of the above-men-

Table 1 Historical overview: the development of CT

1895	W.C. Roentgen discovers “a new kind of rays”, later referred to as “X-rays” or ‘roentgen rays’ in his honor.
1917	J. H. Radon develops the mathematical foundation for reconstructing cross-sectional images from transmission measurements [Radon, 1917].
1963	A.M. Cormack describes a technique for calculating the absorption distribution in the human body [Cormack, 1963].
1972	G.N. Hounsfield and J. Ambrose conduct the first clinical CT examinations [Hounsfield, 1973].
1974	60 clinical CT installations (head scanners).
1975	First whole-body CT scanner in clinical use.
1979	Hounsfield and Cormack awarded the Nobel Prize.
1989	W.A. Kalender and P. Vock conduct the first clinical examinations with spiral CT [Kalender, 1989; Kalender, 1990b].
1998	Introduction of multi-slice scanners (four slices).
2000	Introduction of combined PET/CT systems.
2001	Introduction of 16-slice scanners.
2004	Introduction of 64-slice scanners.
2006	Introduction of dual-source CT.
2010	More than 50,000 clinical CT installations (whole body scanners) worldwide.

tioned earlier findings. His success took the entire medical world by surprise, and he achieved his remarkable breakthrough neither at a renowned university nor with a leading manufacturer of radiological equipment, but with the British firm EMI Ltd. His invention gave EMI, which had until then manufactured only records and electronic components, a monopoly in the CT market that lasted for 2 years, and the terms “EMI Scanner” and “CT Scanner” became almost synonymous. In 1974 Siemens became the first traditional manufacturer of radiological equipment to market a head CT Scanner, after which many other companies quickly followed suit. A boom followed, reaching its peak in the late seventies with 18 companies offering CT equipment. Most of these, including EMI, have withdrawn from the market by now.

The first clinical CT images were produced at the Atkinson Morley Hospital in London in 1972. The very first patient examination performed with CT offered convincing proof of the effectiveness of the method by detecting a cystic frontal lobe tumor. CT was immediately and enthusiastically welcomed by the medical community and has often been referred to as the most important invention in diagnostic radiology since the discovery of x-rays; its later development only confirmed these early expectations. Computed tomography has become a very important factor in radiological diagnosis. While only 60 EMI scanners had been installed by 1974, there were more than 10,000 devices in use in 1980, including a high number of head scanners. In 1979 Hounsfield and Cormack, an engineer and a physicist, were awarded the Nobel Prize for medicine in recognition of their outstanding achievements.

At this point, the development seemed to have reached its peak, and the eighties saw scarcely any technological progress. The introduction of spiral CT in 1989 [Kalender, 1990b] and the following developments in x-ray, detector and scanner technology have led to a renewal of interest in clinical applications. For the year 2010, the number of clinical installations in operation is estimated to be above 50,000, almost exclusively whole-body scanners. The upward trend is unbroken for the time being, and the position of CT is consolidated despite further developments in other radiological methods.

1 Principles of Computed Tomography

1.1 General Considerations on Slice Imaging

CT was the first widely used radiological imaging modality which exclusively provided computed digital images instead of the well known directly acquired analog images. And it offered images of single discrete slices instead of superposition images of complete body sections. The two characteristics “digital” and “volume representation by single slices”, which were new at the time, are in the meantime familiar and are also associated with other slice imaging modalities such as ultrasound, magnetic resonance tomography (MRT) and positron emission tomography (PET). Are there any limitations or disadvantages associated with these two characteristics? What advantages do they offer? In the section following below a short discussion of the principal considerations is offered for the interested reader. It will be shown that the characteristics “digital” and “volume representation by single slices” are hardly noticeable these days and that contrast which is defined locally for slice images constitutes the decisive principal difference compared with conventional x-ray imaging. Readers familiar with medical imaging in general and with CT may possibly glance over the figures only or immediately continue with section 1.2 or chapter 2, respectively.

1.1.1 Computed Tomography – a Digital Modality

We have been familiar with radiographs, i.e. imaging of parts of the human body by means of x-rays and film, for more than a century now. Anatomy is presented on the analog medium film as a continuum with almost arbitrary fine transitions, similar in this respect to photographic pictures on film. The human eye does not recognize any steps in intensity or discrete picture elements. Intuitively one assumes that arbitrarily fine gradations of gray levels and continuous transitions for contours are given. The situation is similar to the hearing process: the human ear subjectively perceives a continuous frequency spectrum when listening to music or arbitrary natural sounds. In both cases – in visual and in auditory perception – analog recordings are classified as “arbitrarily fine”, while digital is often associated with “coarse or discrete sampling”.

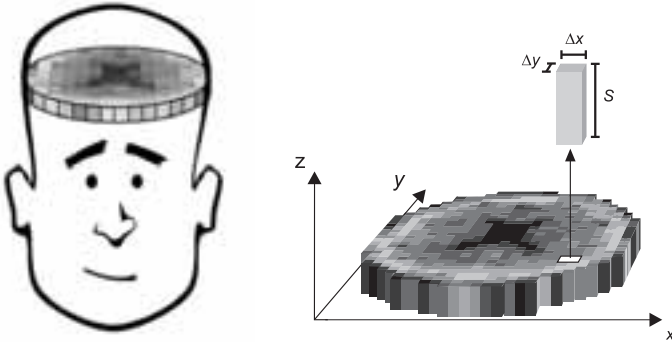


Figure 1.1

Computed tomography – perception in slices. CT provides transverse slice images of the human body in digital form. A coordinate system then results which basically conforms to the anatomical main axes and planes.

Today we have come to recognize and accept – and with respect to the example of audio records, even most admirers of good old analog records do so as well – that the same high recording and perception quality can be made available with digital media. For CT, this was definitely not the case in the early days.

For an understanding of computed tomography it may be helpful to view the human body as built up of a finite number of discrete slices and volume elements. Each single scan aims to determine the composition of one transverse cross-section. This respective slice or section can be imagined in turn as composed of discrete cubic volume elements (figure 1.1). The value attached to each volume element is displayed in one picture element of the digital image matrix. For volume elements we often use the acronym “voxel”, and for picture elements the term “pixel”.

In principle, a slice image can be generated in arbitrary orientation. For CT, however, mostly a transverse plane here labeled as the x/y -plane is scanned directly. The z -axis, oriented perpendicular to the scan and image plane, is thereby aligned along the axis of rotation of the scanning system and thus approximately parallel to the body’s longitudinal axis (figure 1.1). Sagittal body sections are approximated by y/z -planes, and coronal sections by x/z -planes.

The edge lengths of a voxel in this coordinate system are determined by the pixel size, resulting from the selected matrix size and field of view (see section), and the slice thickness S . For coarse matrices, a chess-board-like impression may result. This was in fact the case for early CT images which

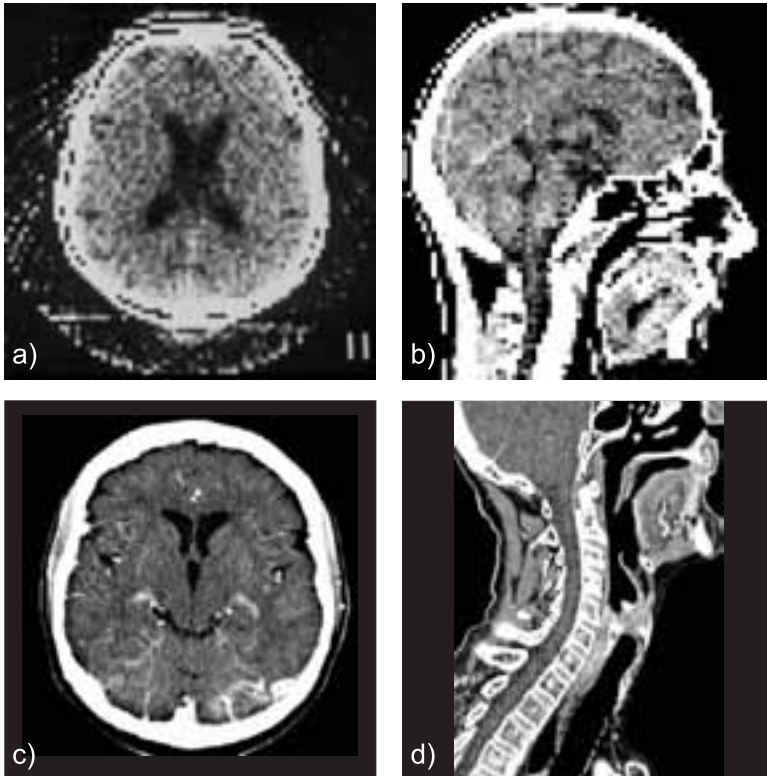


Figure 1.2

Analog or digital images? Continuous imaging of anatomy or scanning of single slices? In early CT images, here a brain scan produced in 1974 with an 80×80 image matrix (a), the computed discrete picture elements are clearly visible, just as the steps in the secondary reconstructions generated from single scans taken with a spacing of 13 mm (b). For volume scans obtained in spiral scanning mode and reconstruction of finer matrices (c) picture elements cannot be discerned from analog images anymore; they can also be viewed in the third dimension quasi-continuously (d).

were reconstructed, fully adequate for the low spatial resolution at that time, with an 80×80 matrix (figure 1.2a). The impression is disturbing, however; the quality of such a digital image is obviously still limited. Multi-planar representations in planes perpendicular to the scan plane also exhibit a coarse appearance depending on the slice thickness (figure 1.2b). These limitations in image quality are not of a fundamental nature; they result from limitations in the techniques used.

The chapters following below will further illustrate that the question “analog or digital?” does not bear high relevance for CT imaging anymore, as it was

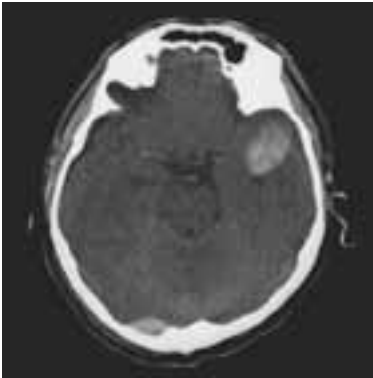
the case in the early days of CT (figure 1.2a,b). Matrix sizes and spatial resolution for the imaged slice have reached values which hardly allow a differentiation – no matter whether the image has been generated quasi in an analog manner or built up from discrete picture elements (figure 1.2c). The image remains digital in nature of course; pixels can be made visible by high magnification of any arbitrary image. This can be verified by a simple exercise using the magnify function in the evaluation software on the enclosed DVD.

Only for the third dimension, along the z -axis in our coordinate system, can the effects of low spatial resolution and large slice thickness often still be recognized. Choosing thin slice widths and overlapping image reconstruction for spiral CT or multi-slice spiral CT scans meanwhile provides the quality of analog images to a good approximation (figure 1.2d). Digital images with their computed discrete picture elements, which have come into broad use in radiology through CT, do not entail any disadvantages.

1.1.2 Why Do Slice Images Offer Higher Contrast?

Conventional film radiography offered a valuable non-invasive means of diagnosis for many decades. Its limitations were and are severe, however; we are increasingly less aware of these due to the availability of alternative procedures. Imaging the brain by radiographs, for example, yields insufficient results in most cases. Roentgenologists tried to solve this dilemma by various measures, for example by using contrast media such as air in pneumoencephalography. In spite of the high efforts and the great discomfort to the patient these procedures only yielded very limited additional information. Computed tomography for the first time offered the possibility to image brain structures in diagnostic quality with high contrast (figure). How is this achieved? Several radiological text books offered the explanation that the high contrast of CT images is due to the higher dose. This explanation is wrong. Although both radiography and CT use x-rays, CT images display a quantity different from that in radiographs.

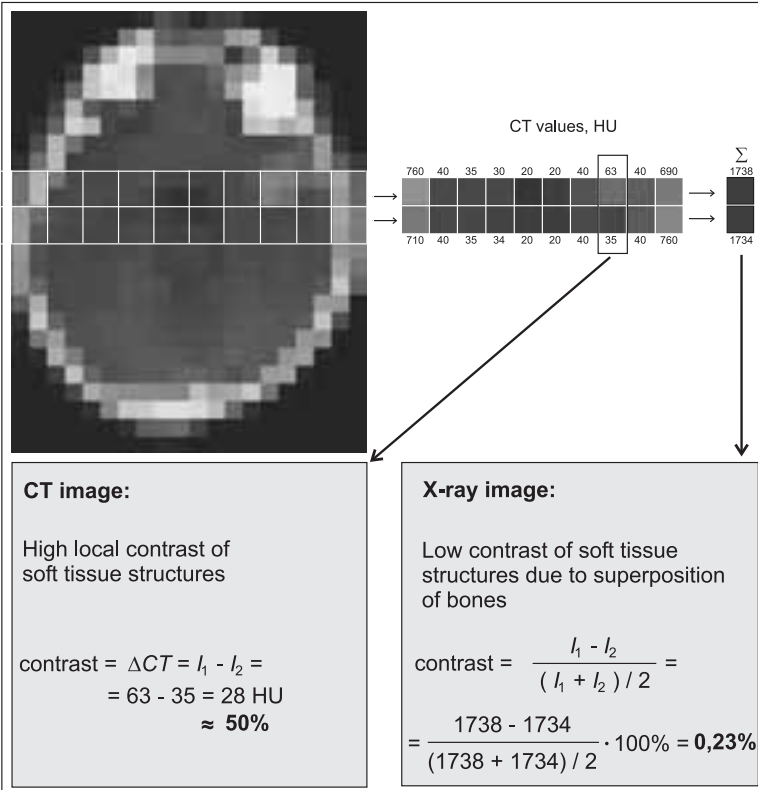
The principle of radiography is to record the radiation which is emitted from the focus of an x-ray tube and attenuated by the object to be examined with a detector, traditionally by film. Thus, a conventional radiograph presents the modulated distribution of radiation intensity and always offers a superposition image: all structures along the rays from x-ray focus to detector, i.e. all volume elements passed by any ray, contribute to the attenuation of the radiation intensity. Each picture element displays the sum of all contributions to attenuation or, mathematically speaking, the integral of the attenuation components along a line. We will return to these “line integrals” again when discussing the principle of computed tomography in the next section.



a)



b)



c)

◀ Figure 1.3

Why does CT offer higher contrast? **a)** CT images display the attenuation resulting from each volume element directly assigned to the respective single picture element. Accordingly, contrast in CT is defined by local differences in attenuation and the lesion is easily recognized. **b)** Projection images, in this case the conventional radiograph of the skull, render the sum of all signal contributions along a ray from the x-ray source to each picture element. In such a superposition image, only structures can be recognized which exhibit very high differences in attenuation with respect to their surroundings. **c)** The high contrast offered by CT images – here illustrated by way of numbers as an arbitrary example only – is due to the imaging principle and not due to radiation dose or scan parameters.

Image contrast is defined by the difference in intensity of two neighboring picture elements or regions. This definition holds true in the same way for conventional radiographs and for CT images. Contrast in radiographs is dominated by structures with high attenuation such as bone and contrast media or by differences in object thickness. Contributions from structures with low attenuation, typically soft tissue structures, are thereby completely hidden in most practical cases. This fundamental problem in conventional imaging cannot be eliminated. Even the introduction of improved detector systems or digital data processing or an increase of dose will not alter the situation.

For slice images contrast is given directly by the attenuation values of neighboring volume elements or subvolumes and not by line integrals representing a path through the complete object. Contrast is determined locally by the composition of the tissues, while neighboring or superimposed structures have no or only very little influence. Arbitrarily small differences in the density or the composition of tissues can therefore be rendered with sufficient contrast as a matter of principle. This statement is true for all slice imaging modalities. This decisive advantage of slice imaging, illustrated in an exemplary fashion in figure c, led to the immediate breakthrough of CT with its introduction in the year 1972.

1.2 Basic Principles of CT

In general terms, the principle of computed tomography consists of measuring the spatial distribution of a physical quantity to be examined from different directions and to compute superposition-free images from these data. This abstract principle will be illustrated for sequential CT, i.e. the scanning of single slices, in an illustrative way by answering the questions following below. The underlying mathematical foundations will be left out as much as

possible. A short description of these is offered in chapter 9.2; detailed elaborations are found in the literature, for example in [Brooks, 1976a; Scudder, 1978; Morneburg, 1995].

1.2.1 What Do We Measure in CT?

For survey radiographs, the relative distribution of the x-ray intensity is recorded; i.e. for classical radiographs only the gray value pattern is utilized to derive a diagnosis. In CT, the intensity of x-rays is also recorded behind the object. In addition to the intensity I attenuated by the object, the primary intensity I_0 has to be measured in CT to calculate the attenuation value along each ray from source to detector. The respective formula and some simple cases are illustrated in figure 1.4.

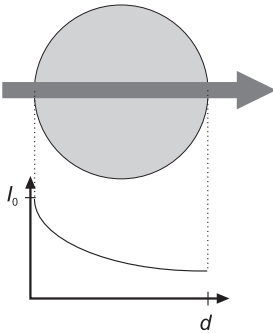
The simplest case is given by a measurement of a homogeneous object with monochromatic radiation (figure 1.4, case 1); this case does not necessarily demand tomographic imaging, but it is familiar to us from many different measurement procedures. The intensity falls off exponentially with absorber thickness. Attenuation, defined as the natural logarithm of the ratio of primary intensity to attenuated intensity, is given in this case in a simple manner as the product of the linear attenuation coefficient μ and the absorber thickness d . If the absorber thickness is known μ can be determined directly. The distribution of μ along the ray path remains unknown, however.

Case 2 in figure 1.4, representing a simple inhomogeneous object, is of greater interest. The contribution to total attenuation resulting from each ray path interval depends on the local value of the attenuation coefficient μ_i . Summation over the path intervals, even for simply structured objects, has to be carried out in general with small increments d_i and therefore can be expressed as the integral over μ along the ray path. CT consists of measuring many such line integrals exactly. Radon showed in his early work [Radon, 1917] that the two-dimensional distribution of an object characteristic can be determined exactly if an infinite number of line integrals is given. A finite number of measurements of the distribution of the attenuation coefficient $\mu(x,y)$ is sufficient to compute an image to a good approximation. A single measurement only, as given in projection radiography, will not allow us to solve for μ_i in case 2 or for the distribution $\mu(x,y)$ in general.

Figure 1.4 ►

What do we measure in CT? The intensity I of radiation. The attenuation value, i.e. the projection value P , results and thus, in the simplest case, the attenuation coefficient μ (case 1). For inhomogeneous objects tomographic imaging is necessary to determine the distribution $\mu(x,y)$.

Case 1: homogeneous object, monochromatic radiation

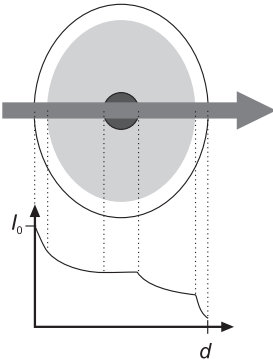


$$I = I_0 \cdot e^{-\mu \cdot d}$$

$$P = \ln \frac{I_0}{I} = \mu \cdot d$$

$$\mu = \frac{1}{d} \cdot \ln \frac{I_0}{I}$$

Case 2: inhomogeneous object, monochromatic radiation

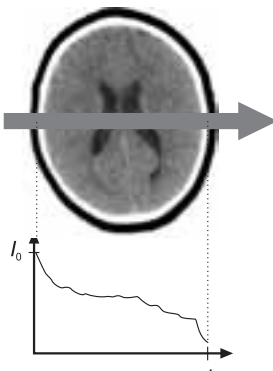


$$I = I_0 \cdot e^{-\mu_1 \cdot d_1 - \mu_2 \cdot d_2 - \mu_3 \cdot d_3 - \dots} = I_0 \cdot e^{-\left[\sum_{i=1}^n \mu_i d_i\right]} = I_0 \cdot e^{-\int_0^d \mu ds}$$

$$P = \ln \frac{I_0}{I} = \sum \mu_i d_i$$

$$\mu_i = ?$$

Case 3: inhomogeneous object, polychromatic radiation



$$I = \int_0^{E_{\max}} I_0(E) \cdot e^{-\int_0^d \mu(E) ds} dE$$

$$P = \ln \frac{I_0}{I}$$

$$\mu(x, y) = ?$$

Before explaining how the measurement has to be carried out and how an image can be computed it must be said that the linear attenuation coefficient may depend strongly on energy. In measuring intensities – and this is done automatically in today’s CT systems – we also integrate over all energy intervals as illustrated for case 3 of figure 1.4. The dependence on energy may yield problems, above all beam hardening effects, which will be discussed in chapter 4. However, this can also be used to advantage in dual energy methods for material-selective measurements. If we also consider a potential dependence of attenuation on time, the measured quantity in CT, the linear attenuation coefficient is given as $\mu(x,y,z,E,t)$. A dependence of μ on time can be generated by the administration of contrast media or be given by physiology, for example in lung tissue as a function of inspiratory volume. In the following sections we will focus on the simple case of measuring and computing $\mu(x,y)$ only for a given slice position z .

1.2.2 How Do We Measure an Object in CT?

To be able to compute an image in acceptable quality following Radon’s theory, a sufficiently high number of attenuation line integrals or projection values have to be recorded. It is necessary to carry out measurements in all directions, i.e. at least over an angular range of 180° , and to determine many narrowly spaced data points for each projection.

A simple measurement setup fulfilling this purpose is sketched in figure 1.5. A radiation source with adequate collimation emits a pencil beam and the intensity, attenuated by the object, is registered by the detector placed opposite. For a given angular position, this setup of radiation source and detector is moved linearly (translation), and the intensity is measured either at single discrete points or continuously. This results in an intensity profile recorded for parallel rays. By determining the ratios of the primary intensity recorded in the periphery and the attenuated intensities recorded behind the object and taking their logarithms, an attenuation profile results which is generally termed a projection. Projections are measured successively for successive angular positions. The complete set of projections, here determined in parallel ray geometry over 180° , is then transferred to the data processing unit. Exactly this procedure was used in the first clinical CT scanners, with 180 projections taken in 1° angular intervals (stepwise rotation) with 160 data points measured per projection.

CT scanners today measure typically in fan-beam geometry over an angular range of 360° . The extension to 360° resulted from several considerations, initially focussing on image quality and better data sampling. By proper geometrical alignment of the detector, the quarter detector offset, overlapping sampling is achieved (see section 2.2.1). Practical considerations also

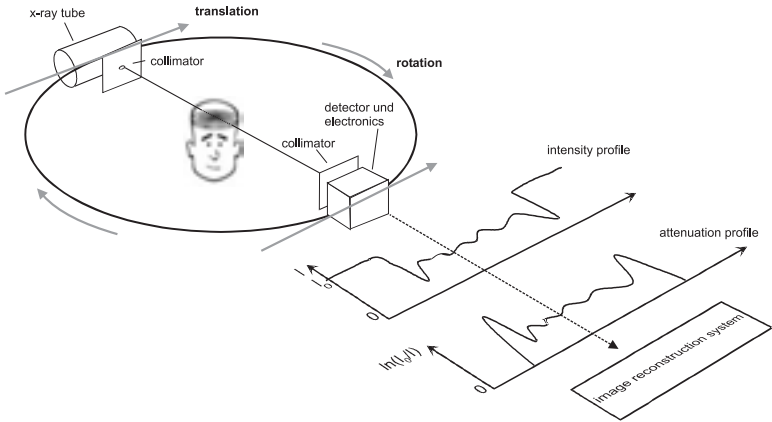


Figure 1.5

How do we measure an object in CT? In the simplest case x-ray intensities and therefore object attenuation will be measured with a pencil beam for many different angular positions.

demand 360° scanning; for spiral CT in particular, this is a prerequisite. Modern CT scanners typically measure 800-1,500 projections with 600-1,200 data points per projection.

1.2.3 How Do We Compute a CT Image?

Information on the as yet unknown distribution $\mu(x,y)$ of attenuation coefficients is only given in form of a set of projection values, which is also termed the “Radon transform” of the image. An inverse transformation has to be carried out to determine $\mu(x,y)$. Different procedures are available to do this. The most easily understood approach to solve this problem is the following: N^2 unknown values, the $N \times N$ pixel values of the matrix, have to be computed by solving N_x independent equations, the measured projections. If N_x , the product of the number of projections N_p times the number of data points per projection N_D , is larger than or equal to N^2 this is possible.

In the simplest case of an image matrix with only four pixels (2×2 matrix) two measurements for two projections will yield a system of four equations and four unknowns which can be solved easily (figure 1.6). The extension to a 3×3 matrix with nine unknowns can also be solved easily with twelve measured values given as assumed in this schematic representation. These so-called algebraic reconstruction techniques (ART) were actually used in the early days of CT, as for example in computing the image in figure 1.2a as a 80×80 matrix. The image was computed in an iterative fashion, i.e. by

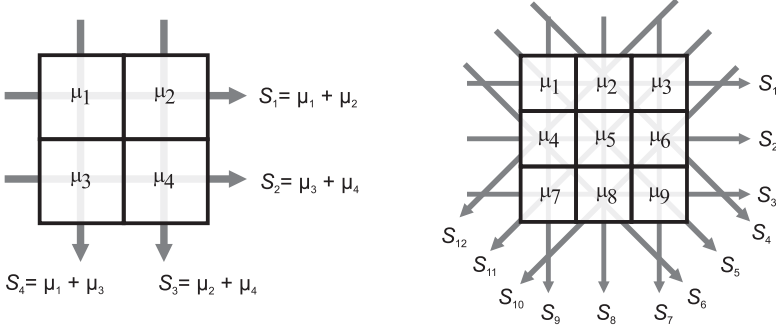


Figure 1.6

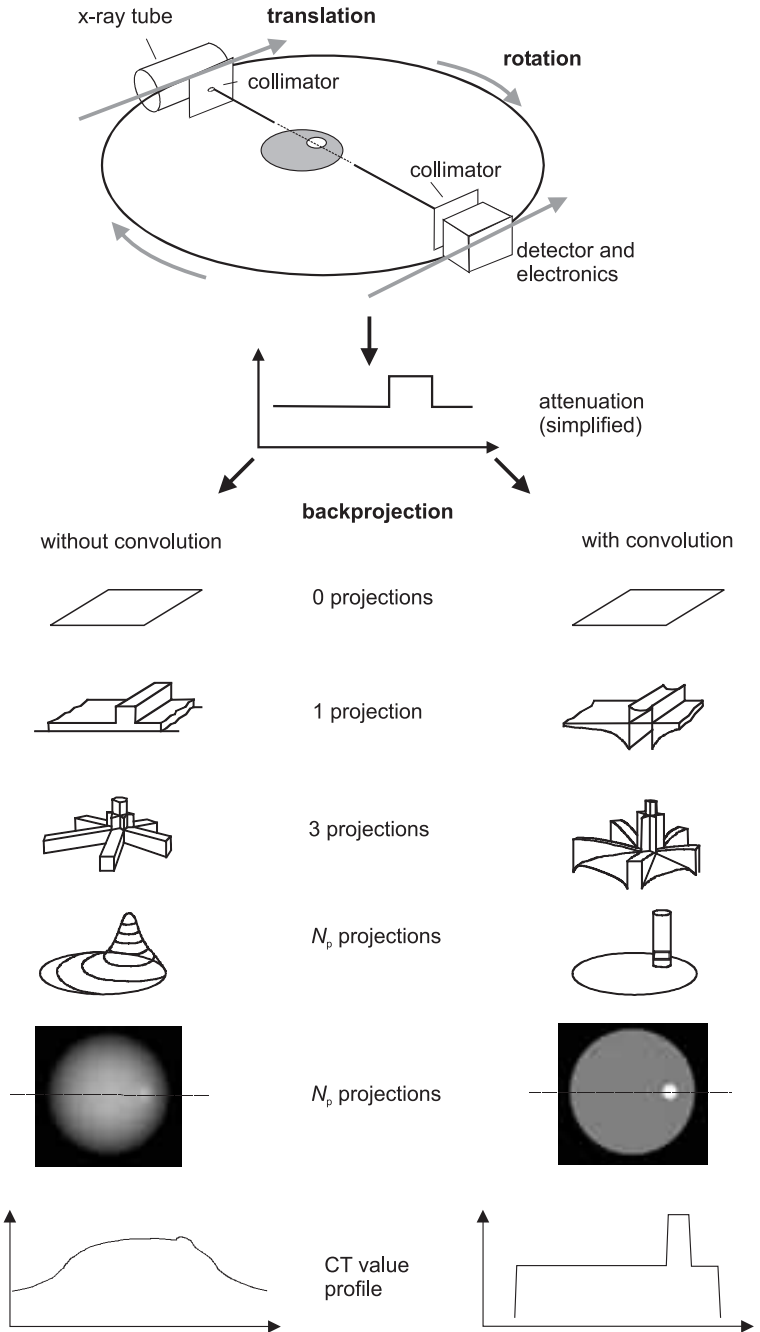
How do we compute a CT image? Algebraic procedures are the most easily comprehensible approach to image reconstruction. The N^2 unknown values of an $N \times N$ image matrix can be determined by solving a system of linear equations. For larger matrices this has to be done iteratively.

repeating the calculation in an effort to improve accuracy with each step. For larger data volumes, finer image matrices and the higher demand on image quality ART approaches led to unacceptably high computation times.

In today's CT scanners the so-called convolution-backprojection procedure is usually utilized. This is illustrated in figure 1.7. The respective considerations are illustrated additionally by video clips on the DVD which demonstrate the process of image formation in CT. The starting point is always an empty image matrix, i.e. a defined range of computer memory which contains only zeros as starting values. For simple backprojection each projection value is added to all the picture elements in the computer memory along the direction in which it has been measured. (It is possible to reconstruct only a part of the object as a zoom reconstruction. This may improve spatial resolution, as will be discussed in section 4.1.3.) In general, each detail in the object and represented in the attenuation profile does not only contribute to the pixel value at the desired image point, but to the entire image as well. Even when considering only three projections it becomes apparent that an unsharp image will result. For the very simple object in figure 1.7, the origin of the single image detail is easily recognized, since the image intensity is highest here. The display is unsatisfactory, however, as can be seen in figure

Figure 1.7 ▶

Image reconstructions in CT by convolution and backprojection. Direct backprojection of attenuation profiles results in unsharp images. Convolution of attenuation profiles before backprojection, essentially a high pass filtering, counteracts this unsharpening. (See also the video clips on the DVD)



1.7 at the lower left, which represents the result for the chosen object in an actual measurement and reconstruction. The far-reaching signal contributions due to the backprojection process lead to an unsharp image, which is insufficient for the diagnosis of complex structures.

To avoid this unsharpening each projection has to be convolved before back-projection with a mathematical function, the convolution kernel. This constitutes a pointwise multiplication of the convolution kernel and the attenuation profile and addition of the resulting values (for mathematical definitions see chapter 9.2). In essence, this represents a high pass filtering procedure which generates over- and undershoots at object boundaries. For a positive signal, negative undershoots are generated. These negative contributions will even out the far-reaching positive signal contributions outside each object detail due to the backprojection procedure (figure 1.7 lower right). Convolution additionally offers the possibility to influence image characteristics by the choice and design of the convolution kernel – from soft or smoothing to sharp or edge enhancing (figure 1.8). A relatively weak highpass filter reduces spatial resolution as well as image noise, a strong high pass filter has the opposite effect, as will be discussed further in chapter 4.

Fourier methods offer a further procedure for image reconstruction which is mathematically equivalent to the convolution-backprojection approach.

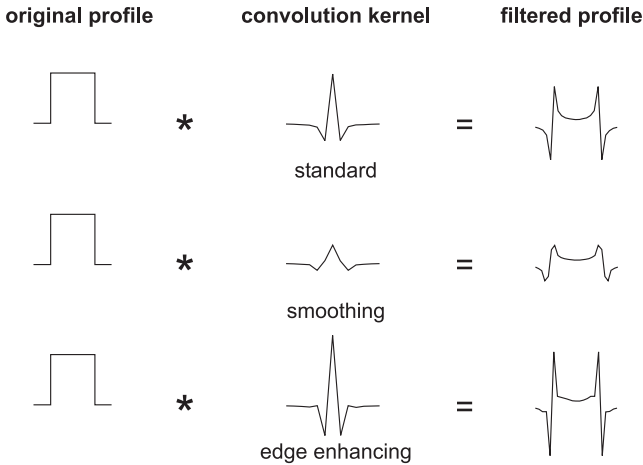


Figure 1.8

Image characteristics can be influenced by the choice of the convolution kernel, whereby increasing spatial resolution or edge enhancement also means increasing image noise.

Convolution and backprojection can be considered the method of choice for CT image reconstruction until today. The iterative ART approach described above was not considered for practical use in CT for the last three decades, but this may gain in importance in the future as faster and less costly computer components become available. IRIS, ASIR, MBIR and other approaches have become hot topics with the “IR” in their names indicating “iterative reconstruction”. The underlying principles are reviewed briefly in chapter 8 with application examples shown.

1.2.4 What Is Displayed in CT Images?

As explained above, CT measures and computes the spatial distribution of the linear attenuation coefficient $\mu(x,y)$. However, the physical quantity μ is not very descriptive and is strongly dependent on the spectral energy used. A display of μ would make quantitative statements cumbersome; a direct comparison of images obtained on scanners with different voltages and filtration would be limited. Therefore, the computed attenuation coefficient is displayed as a so-called CT value relative to the attenuation of water (figure 1.9). In honor of the inventor of CT, CT values, often also referred to as CT numbers, are specified in Hounsfield units (HU). For an arbitrary tissue T with attenuation coefficient μ_T the CT value is defined as

$$\text{CT value} = (\mu_T - \mu_{\text{water}}) / \mu_{\text{water}} \cdot 1000 \text{ HU} \quad (1.1)$$

On this scale, water and consequently each water-equivalent tissue with $\mu_T = \mu_{\text{water}}$ has the value 0 HU by definition. Air corresponds to a CT value of -1000 HU, since $\mu_T = \mu_{\text{air}}$ is equal to zero to a good approximation. The CT values of water and air are independent of the energy of the x-rays and therefore constitute the fixed points for the CT value scale.

Lung tissue and fat exhibit negative CT values due to their lower density and the resulting lower attenuation ($\mu_{\text{lung}} < \mu_{\text{water}}$). Most other body areas exhibit positive CT values, due to the physical density of muscle, connective tissues and most soft tissue organs. For bone and calcifications the higher effective atomic number of calcium, in addition to increased density, is responsible for increased attenuation and therefore for higher CT values of typically up to 2000 HU. CT values of bone or contrast media are more strongly dependent on x-ray energy than water and increase with reduced high voltage settings, which conforms to the contrast behavior in conventional radiographs in principle.

The Hounsfield scale has no upper limit. For medical scanners a range from -1024 HU to $+3071$ HU is typically provided. Consequently, $4096 (= 2^{12})$ different values are available and 12 bits per pixel are required. Image recon-

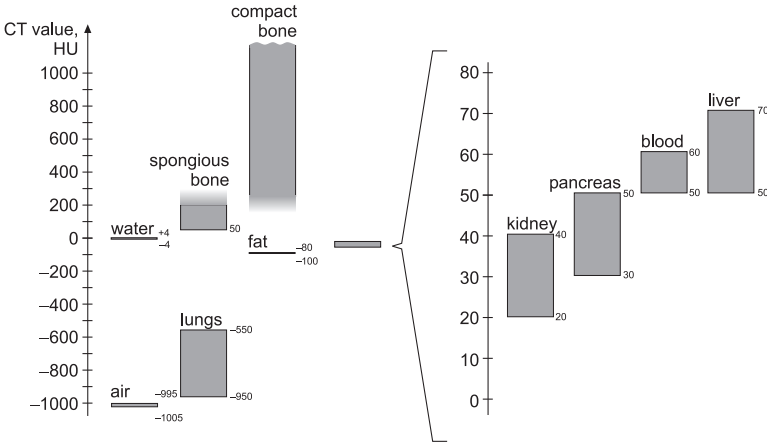


Figure 1.9

The Hounsfield scale. CT values characterize the linear attenuation coefficient of the tissue in each volume element relative to the μ -value of water. The CT values of different tissues are therefore defined to be relatively stable and to a high degree independent of the x-ray spectrum.

struction with an extended scale, which is of particular interest for industrial applications, can also be of value in special medical applications. Imaging bone and measuring its density and structure in the vicinity of metallic endoprotheses constitutes one example.

Windowing

The CT value range from -1024 HU to $+3071$ HU, i.e. 4096 gray levels, cannot be evaluated or differentiated in a single view, neither on a monitor nor by documentation on film. Human observers can typically discern up to a maximum of 60 to 80 gray levels. Therefore, the complete gray scale is assigned to the CT value interval of interest only, the so-called window; values above the chosen window will be displayed as white, and the values below the window as black. This procedure, the so-called windowing, is carried out on the CT console interactively and without time delay. To choose the desired CT value interval only the center and the width of the window have to be adjusted by mouse, potentiometer or a similar device. The center is chosen corresponding approximately to the mean CT value of the interesting structures, while the window width determines the contrast in the image. For the display of very small attenuation differences as given in the brain, for example, a narrow window is chosen. For large differences, as presented by the lung or the skeleton, for example, a wide window is chosen (figure 1.10).

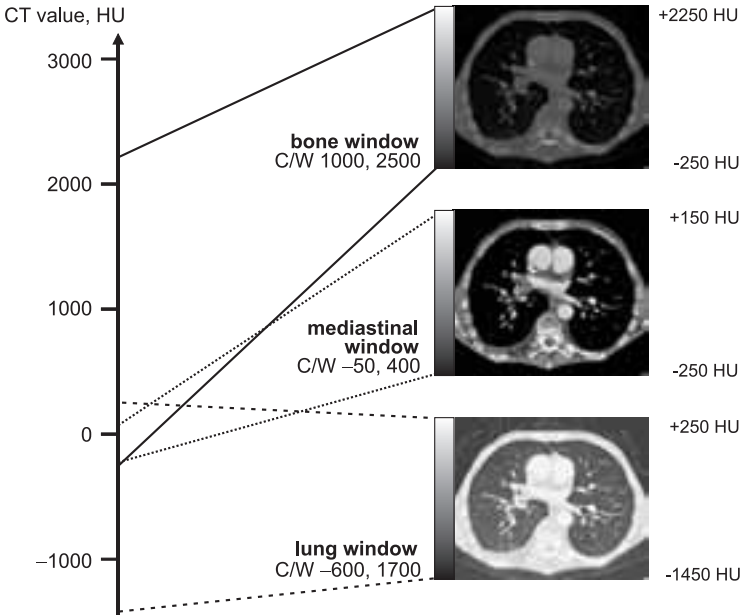


Figure 1.10

Windowing procedures to display CT images. The diagnostically relevant range of CT values is selected by choosing the center and width (C/W) of the window. The complete gray value scale is assigned to this selected range only for display on a monitor or film.

Examples have been compiled for illustration on the DVD for readers who have no access to a CT scanner or to an evaluation station; these readers can interactively explore the effects of changing window settings using the software package offered there.

Significance of CT numbers

CT values can be interpreted in a simple and in most cases unambiguous way. An increase in CT values can be assigned to increased density and/or an increase in effective atomic number. This corresponds to the physical definition of the linear attenuation coefficient

$$\mu = \left(\frac{\mu}{\rho} \right) (E, Z) \cdot \rho \quad (1.2)$$

μ is the product of the density ρ and the mass attenuation coefficient μ/ρ which depends on the energy E of the x-rays used and the atomic number Z

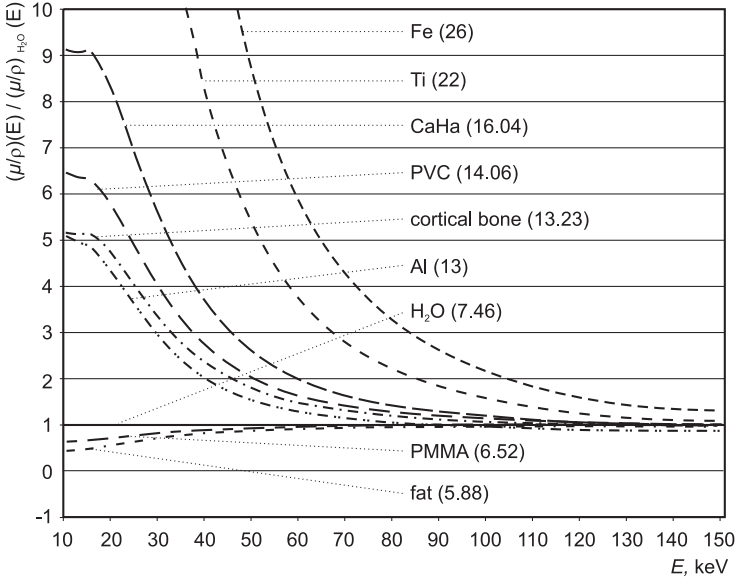


Figure 1.11

Mass attenuation coefficients of different materials relative to those of water; effective atomic numbers are given in parentheses. CT values are increased when the atomic number or the density of the material are higher than that of water.

of the material or tissue in question. Values of the mass attenuation coefficient as a function of energy are shown in figure 1.11 for several elements and materials relative to the values for water. This illustrates that CT value differences due to effective atomic numbers decrease for higher energies. Contrast at high energies is dominated by density differences. This holds true for tissues of high atomic number, such as bone, in the same way as for tissues with low atomic numbers, such as fat. The negative contrast of fat, typically -80 to -100 HU, is caused both by the low effective atomic number Z_{eff} of approximately 5.88 and by the low density of approximately 0.96 g/cm^3 .

For the interpretation of CT values it must also be considered that the contribution of all materials or chemical elements in a given voxel are averaged. The explanation of why attenuation and thus CT values increase or decrease is nevertheless not a problem in most cases and apparent for experienced radiologists.

However, there may also be unclear findings, for example the question if a region with increased attenuation in soft tissue represents a fresh process



Figure 1.12

Principle and results of dual energy CT. The area of increased CT values in the standard CT image can be interpreted correctly by means of material density images: soft tissue density is increased, there is no calcium deposit [Kalender, 1987c].

corresponding to bleeding or an old process which is diffusely calcified. In such cases, dual energy CT can clarify the situation (figure 1.12).

Dual energy CT makes use of the energy dependence in μ due to the materials' atomic numbers. In general, two scans with different spectra are carried out and the attenuation values and the differences in attenuation for the two spectra have to be evaluated. Different approaches are available for this purpose. The aim is always to generate material-selective images and to determine material density as accurately as possible. Implementations which are based on the measured attenuation integrals and the principle of base material decomposition can provide images of calcium and soft tissue density (figure 1.12) as well as images of electron density, effective atomic number and so-called monoenergetic images free of beam hardening effects [Kalender, 1987a]. The only dual energy CT product available in the past was offered for several years on Siemens scanners of the SOMATOM DR type and

was used especially for the highly accurate measurement of bone mineral density in the lumbar spine [Kalender 1987c]. The high technical effort was not considered adequate for many years. Followed by the introduction of dual source CT (see section 2.4.5), dual energy methods became of interest again with several technical solutions being presented and quite a number of applications being accepted. Therefore dual energy methods are covered in some detail in the separate new section 7.4.

2 Technical Concepts

2.1 Phases of Development and Goals

The technical goals of CT development have continuously been adapted to the technical state of the art and to the topical demands of radiology. One basic demand has always been of high priority: scan times have to be reduced! In addition to other demands such as improvement of image quality, reduction of costs, adaptation of the user interface etc., which always had to be taken into account too, the reduction of scan times appears to have been the decisive trend pursued since the beginning of CT. And it is essential to note that this not just aimed at the speed of taking a single image but at the speed of finishing the complete examination. The performance and the spectrum of applications developed accordingly, driven or accompanied by the necessary improvements in technology. To a good approximation, although not strictly so, the individual phases of development can be assigned to single decades.

2.1.1 The Seventies – from Head to Whole Body Scanning

The development of CT scanners began with Hounsfield's experimental setup, which largely corresponded to the sketch in figure 1.5. This setup has often been termed the "first generation" of CT. The first commercial scanners, the so-called "second generation", differed only little from Hounsfield's scanning system. To speed up scanning detectors were added, which entailed going from a pencil beam to a small fan beam. Both types of scanners functioned according to the translation-rotation principle in which the radiation source and the detector scan the object in a linear translatory motion and repeat this procedure successively after a small rotational increment (figure 2.1a,b). In this manner, Hounsfield sampled 180 projections in 1° steps with 160 data points each, i.e. a total of 28,800 data per scan. This was fully sufficient to calculate an image with 6,400 pixels, i.e. an 80×80 image matrix. Scan times were five minutes; image reconstruction was carried out simultaneously and took the same amount of time. Hounsfield reported an examination time of 35 minutes, in which the dual-row detector acquired 6×2 images with 13 mm slice thickness. This constituted a remarkable performance. In the first trials in 1969 test objects, so-called phantoms,